Energy Conversion and Management 248 (2021) 114783

Contents lists available at ScienceDirect

Energy Conversion and Management

journal homepage: www.elsevier.com/locate/enconman

# Regasification of liquefied natural gas in satellite terminals: Techno-economic potential of cold recovery for boosting the efficiency of refrigerated facilities

Antonio Atienza-Márquez *, Joan Carles Bruno, Alberto Coronas

*Universitat Rovira i Virgili, CREVER – Group of Applied Thermal Engineering, Mechanical Engineering Department, Av. Països Catalans 26, 43007 Tarragona, Spain*

ARTICLE INFO

*Keyword:*
Liquefied natural gas regasification
Satellite LNG terminals
Cold recovery
Energy efficiency improvement
Sustainable refrigeration
Techno-economic potential

ABSTRACT

The regasification of liquefied natural gas releases low-temperature thermal energy, which is usually wasted. Most initiatives to recover this cold mainly focus on large-scale harbour terminals rather than on small-scale applications in satellite facilities. This paper proposes a new system configuration that can be used to exploit liquefied natural gas cold as a by-product of regasification in satellite plants supplying sub-zero refrigeration in agro-food industries. Cold is applied indirectly to lower the condensation temperature of the vapour-compression chillers which handle the thermal load of cold rooms. The system seeks to boost efficiency, an effect that would be more marked in warm climates. Performance is best when the peak refrigeration load matches the maximum cold thermal energy available from the regasification site. When this is the case, the annual electricity saving is 9–22% more than when a conventional refrigeration system is used with wet cooling towers and with no liquefied natural gas cold recovery. The economic potential of the system is assessed with a Monte Carlo analysis. The cost of producing refrigeration throughout the system's lifetime can be reduced by 5–15% with respect to the conventional reference system in warm/temperate locations and for large/medium plant sizes. However, the system is no so competitive in economic terms for cold locations and small-size plants.

## 1. Introduction

Energy transition is crucial in response to one of the major challenges of this century: climate change. The use of low-carbon primary energies and the increase in renewable energies in the energy mix is essential if greenhouse gas (GHG) emissions are to be reduced and global temperatures are to be kept below the limits agreed [1].

However, a drastic transformation of the current energy model (mainly based on oil and coal) is by no means a trivial issue and cannot be addressed overnight. In this regard, natural gas will play a key role as an energy source to transition towards a decarbonized economy largely because its carbon footprint is lower and it emits fewer air pollutants than other fossil fuels. Despite the demand shock caused by the Covid-19 pandemic, the gas trade has shown resilience [2] and the global demand for its cryogenic liquid form (i.e., liquefied natural gas – LNG) has continued to grow [3]. In addition to the benefits of transporting natural gas as LNG instead of using pipelines [4], LNG is an attractive cold thermal energy source because of its very low temperature (111–143 K).

At receiving terminals, LNG is heated up to ambient temperature (regasified) and supplied to final consumers. The cold thermal energy released throughout this process is usually wasted in most regasification terminals worldwide [5], although it can be recovered and used as a by-product for numerous industrial applications [6]. Indeed, there is a considerable amount of literature that discusses how to overcome the barriers to widespread LNG cold utilization [4]. Although most studies have focused on configurations and technologies for power generation [7] as well as on their performance under different working conditions [8]. But there are many other applications beyond electricity generation to use LNG cold, as indicated in [9]. For instance, air liquefaction (e.g., in air separation units [10] or liquid air energy storage, LAES [11]), liquefaction of carbon dioxide ($CO_2$) [12] (e.g., for post-combustion $CO_2$ capture [13]), hydrocarbon separation [14], refrigeration (e.g., warehouses [15], data centres [16] or district cooling networks [4]), desalination [17], hydrogen production [18] and so forth.

Authors have also investigated combining different applications using cascaded polygeneration schemes to extend the efficiency of single-application configurations. For instance, systems for the simultaneous production of power and refrigeration at different temperatures [19], with renewable energy sources [20] and the production of heating

* Corresponding author.
*E-mail address:* antonio.atienza@alumni.urv.cat (A. Atienza-Márquez).

https://doi.org/10.1016/j.enconman.2021.114783
Received 9 July 2021; Accepted 16 September 2021
Available online 8 October 2021
0196-8904/© 2021 The Authors. Published by Elsevier Ltd. This is an open access article under the CC BY-NC-ND license (http://creativecommons.org/licenses/by-nc-nd/4.0/).

**Nomenclature**

*Abbreviations*

| | |
|---|---|
| A1…A10 | Ammonia state points |
| C1, C2 | $CO_2$ state points |
| CTES | Cold thermal energy storage |
| DBHE | Double-bundle heat exchanger |
| EG | Ethylene glycol |
| GHGs | Greenhouse gases |
| HE | Heat exchanger |
| L | Large system size |
| L1…L6 | LNG state points |
| LAES | Liquid air energy storage |
| LHV | Lower heating value |
| LNG | Liquefied natural gas |
| M | Medium system size |
| S | Small system size |
| VCR | Vapor-compression refrigeration |
| W1…WB | Cooling water state points |

*Variables*

| | |
|---|---|
| COEF | Chances of economic feasibility, % |
| Cp | Specific heat, kJ/(kg·K) |
| D | Energy demand, kWh |
| EER | Energy efficiency ratio, W/W |
| EF | Emission factor |
| Ex | Exergy, kJ/kg |
| FCI | Fixed capital investment |
| h | Enthalpy, kJ/kg |
| LCOR | Levelized cost of refrigeration, USD/kWh |
| $\dot{m}$ | Mass flow rate, kg/s |
| p | Pressure, kPa |
| PEC | Purchased equipment cost |
| PLR | Part load ratio |
| $\dot{Q}$ | Heat flux, kW |
| RCI | Refrigeration capacity index |
| s | Entropy, kJ/(kg·K) |
| T | Temperature, K |
| t | Time, s |
| TCI | Total capital investment |
| UA | Overall heat transfer coefficient, W/K |
| V | Volume, $m^3$ |
| $\dot{W}$ | Electric power, kW |

*Greek letters*

| | |
|---|---|
| $\alpha_1 \cdots \alpha_3$ | Refrigeration load factors |
| Δ | Difference |
| $\eta$ | Efficiency, % |
| τ | Temperature factor |
| ξ | Activity factor |

*Subscripts*

| | |
|---|---|
| 0 | Reference environment (exergy calculations) |
| C | Compressor |
| ct | Cooling tower |
| E | Electric output of power plant |
| el | Electricity (consumption) |
| ex | Exergetic |
| IC | Internal combustion engine |
| is | Isentropic |
| m | Mean, motor |
| max | Maximum, peak |
| o | Outdoor |
| ph | Physical (exergy) |
| R | Refrigeration |
| r | Room (indoor space) |
| ref | Reference |

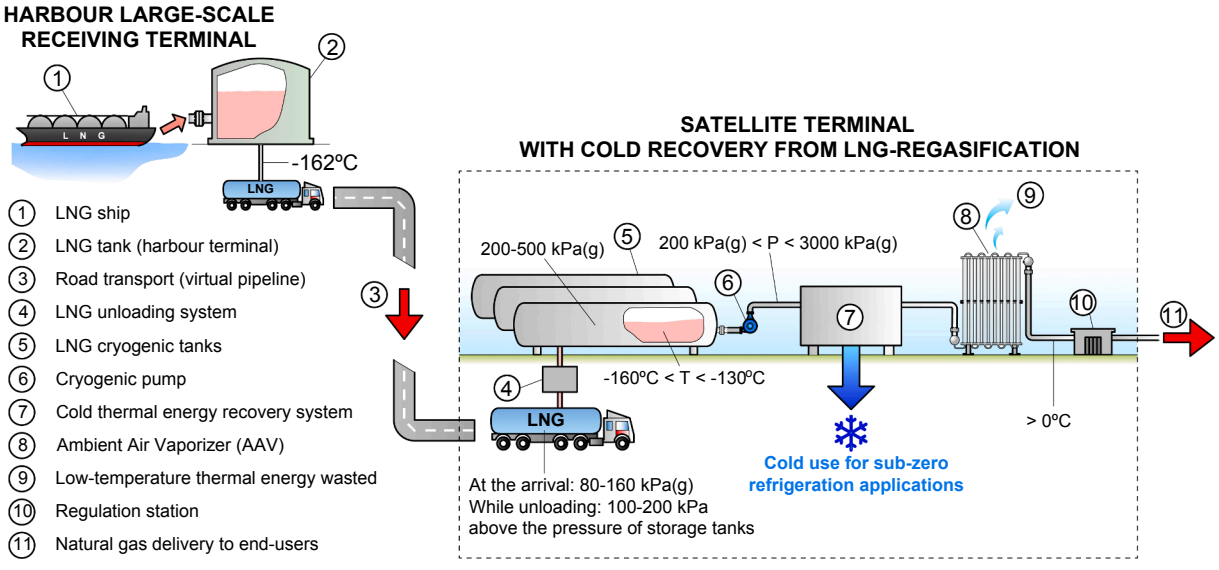


**Fig. 1.** Schematic diagram of the LNG supply chain from harbour terminals to satellite plants recovering cold energy from LNG-regasification.

[21], liquid fuels [22] and many other possibilities. A suitable trade-off between efficiency and simplicity will determine the techno-economic feasibility and the chances for future implementation of LNG-based polygeneration systems [23].

Nevertheless, most of the research on this topic and the very few projects that have already been executed (mostly in Japan) focus on large-scale terminals. In contrast, little research has been done on small-scale cold energy recovery in regasification facilities in areas where

there are no natural gas distribution pipelines. These plants are commercially known as "*satellites*" because they depend on LNG delivered via virtual pipelines (i.e., road, railway, or sea) from a central LNG terminal with a much higher storage capacity (typically, harbour terminals supplied by LNG vessels).

### 1.1. Liquefied natural gas cold recovery in satellite terminals

As illustrated in Fig. 1, and as occurs in large-scale regasification plants, the use of cold thermal energy as a regasification by-product enables the energy consumed in the liquefaction stage to be partially recovered.

Small-scale LNG is an expanding market that facilitates the supply of energy to remote areas or off-grid locations [24], and promotes the integration of renewable energy sources [25] and the development of distributed and more flexible energy systems [26]. Hence, satellite plants support sustainable development and have social benefits because they can provide new job opportunities in rural areas with problems of depopulation and thus contribute to local economies.

The growth in the number of satellite LNG plants is particularly pronounced in China [27]. In Spain there are nearly 900 satellite LNG plants [28] and in Japan there are around ten new satellite plants per annum [29]. Other countries, such as Norway, Netherlands, Turkey, Portugal, or Switzerland, are also active in the small-scale LNG business and it is expanding in South America. As a result, there are thousands of satellite regasification facilities where LNG cold thermal energy could be recovered and, for example, used for refrigeration in adjacent warehouses, thus contributing to the sustainability of their refrigeration systems. It could even be used in the new model of cooling as a service (CaaS [30]). Besides, the deployment of the liquefied biomethane (bio-LNG [31]) industry further promotes the possibility of new satellite facilities with efficient regasification.

To date, however, small-scale LNG cold utilization has been the topic of very little research. Xu et al. [32] proposed a novel air separation process using LNG cold that could potentially be applied in satellite plants. In [33] an optimized analysis was presented of a pioneer demonstration project for storing the cold recovered from LNG-regasification in a satellite plant in China, where the importance of LNG and satellite plants has been highlighted by Lin et al. [34]. Roszak and Chorowski [35] proposed using low-temperature LNG to fill adsorbed natural gas tanks. Ning et al. [36] analysed a small-scale system for the combined production of power and cold at different temperature levels. Kanbur et al. studied various micro-cogeneration systems that used LNG cold: for instance, a micro gas turbine (MGT) system [37] or cycles that combine a MGT with a Stirling engine and thermal energy storage [38], and also with $CO_2$ capture [39]. The authors used finite sum models to forecast the performance of these small-scale configurations [40] and performed life cycle analysis to evaluate their feasibility [41]. Zhao et al. [42] also proposed the use of LNG cold for small-scale $CO_2$ capture applications in the magnesite processing industry.

To the authors' knowledge, the few publications on satellite plants have overlooked the use of LNG cold for refrigeration applications. In a recent doctoral thesis produced by the authors' group entitled "*Exergy recovery from LNG-regasification for polygeneration of energy*" [43], various system configurations mostly engineered for large-scale regasification applications were proposed and analysed. Nonetheless, the thesis also included a chapter on satellite stations. It consisted of a preliminary feasibility study of various configurations and scenarios for exploiting low-temperature LNG for foodstuff refrigeration applications in warehouses located right next to the regasification site. This paper makes a detailed analysis of the case discussed in that thesis that proved to be the most attractive from a techno-economic perspective.

Very few commercial companies engage in activities and initiatives in the small-scale LNG cold recovery business. In 2015 *Kälte-Klima-Sachsen GmbH* [44] built a pilot satellite facility producing 3.3 kW of refrigeration at −50 °C from LNG cold. Its partner company *Eco Ice Kälte GmbH* [45] worked on a regasification system (consisting of a heat exchanger and a brine circuit but no electric compressors) with cold for commercial refrigeration (<100 kW) and freezing and air conditioning applications. Then, in 2018 this business was transferred to *LNGCold Solutions GmbH* [46].

Currently, LNG cold recovery in satellite plants is far from widespread because there are technical and non-technical hurdles that prevent further implementation of LNG cold recovery systems [20]. Some of the most noteworthy, which particularly affect use for foodstuff refrigeration applications, are the following [43]:

- **Less cold thermal energy available** from regasification than in large-scale harbour terminals because of the typically much lower LNG send-out rates (usually < 1 million metric tonnes per annum, MTPA).
- **Higher LNG storage temperature** (see Fig. 1) because of heat gains along the transport chain and during the storage period in cryogenic tanks. This reduces the exergetic potential.
- **Fluctuating gas send-out rate and/or downtime periods** (e.g., due to scheduled maintenance tasks) in most types of satellite plants and, therefore, variable availability of cold thermal energy from the LNG-regasification.
- **Mismatch (in time and amount) between natural gas and refrigeration demand profiles**.

The last two technical issues introduce a dramatic uncertainty as regards the reliability of a system that aims to use LNG cold for refrigeration supply. Since refrigeration outages may break the cold chain of foodstuffs, there is little chance that only the cold thermal energy recovered from LNG-regasification will be sufficient to supply the refrigeration load of cold rooms. Thus, backup refrigeration machines and equipment such as cooling towers will be required regardless of whether LNG cold is recovered or wasted. This damages the economic perspectives. For a standalone configuration consisting only of heat exchangers, the capital investment and maintenance expenses are higher, the energy management is more complex, and the electricity-saving potential is lower [43].

Depending on the type of satellite terminal and the refrigeration needs from neighbouring warehouses in relation to the LNG cold thermal energy available, the factors mentioned above may affect the technical feasibility of using LNG cold thermal energy for refrigeration applications to one extent or another. As far as type is concerned, satellite regasification plants can be classified in terms of how the natural gas supplied will be used and the number of users provisioned. For instance, satellite plants can supply natural gas to industries or electric power plants (i.e., baseload, peak shaving) for mining activities or for the refuelling of vehicles, or they can feed natural gas into the local distribution network of small towns or villages.

In particular, satellite LNG terminals for power plants [47] (with typical electrical power outputs in the range 1–300 MW) are gaining popularity in the small-scale LNG industry. These plants allow for *fuel shifting* from coal/diesel/fuel oil to LNG [48] with a competitive price, lower environmental impact and higher operational flexibility [49], and have the added value that they produce clean refrigeration if the cold from LNG-regasification is recovered [50]. The new energy policies in Indonesia [51] and other insular countries like Greece [52] or the Philippines [53] are based on switching to LNG. The main power plant in Gibraltar (82 MW) is an example of successful fuel shifting from diesel to LNG supplied from a small-scale regasification facility [54].

### 1.2. Objective

This paper addresses the recovery of cold thermal energy from LNG regasification in satellite terminals and its indirect use for refrigerating frozen foodstuffs. The objective is to evaluate the techno-economic

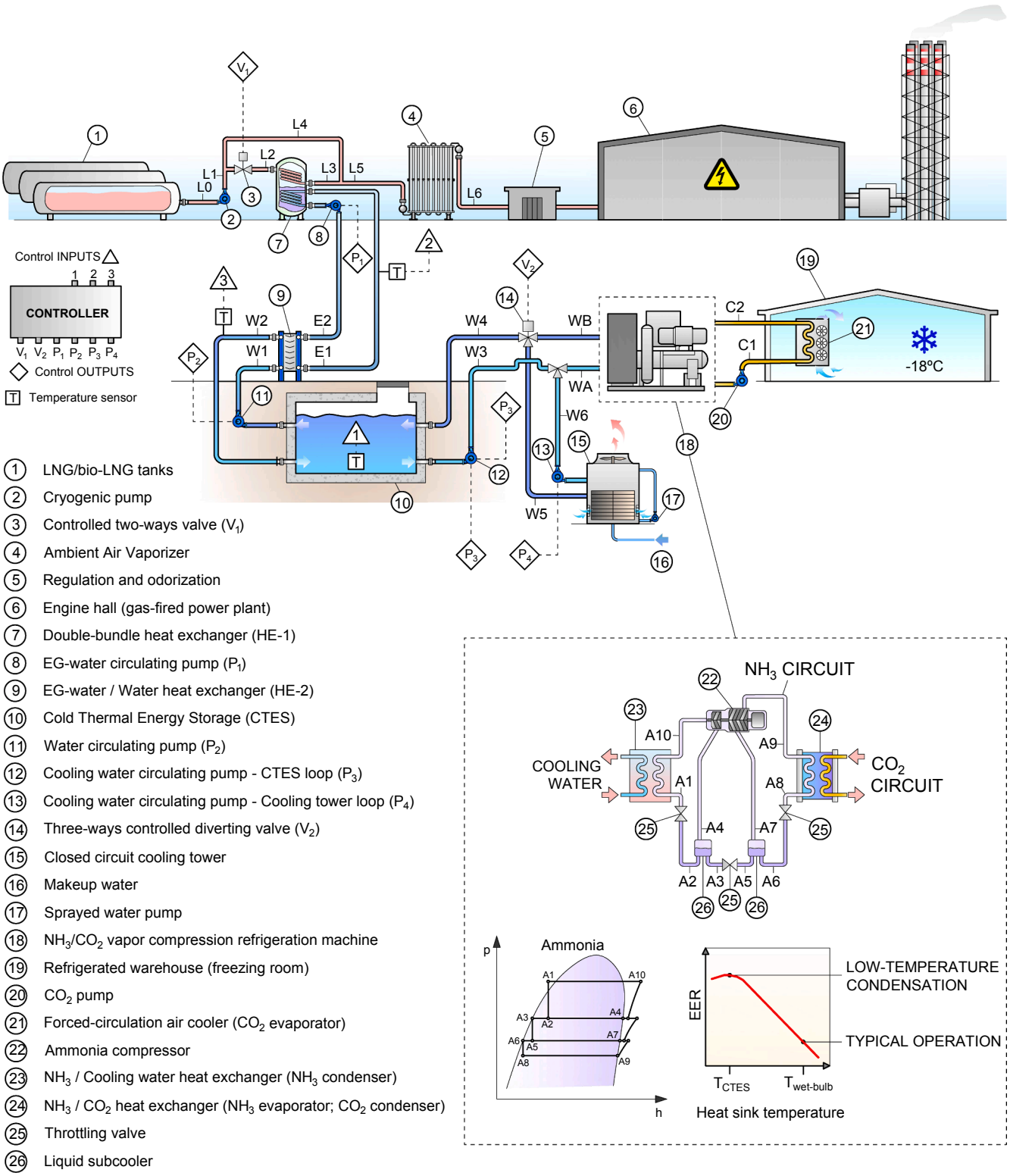


1. LNG/bio-LNG tanks
2. Cryogenic pump
3. Controlled two-ways valve ($V_1$)
4. Ambient Air Vaporizer
5. Regulation and odorization
6. Engine hall (gas-fired power plant)
7. Double-bundle heat exchanger (HE-1)
8. EG-water circulating pump ($P_1$)
9. EG-water / Water heat exchanger (HE-2)
10. Cold Thermal Energy Storage (CTES)
11. Water circulating pump ($P_2$)
12. Cooling water circulating pump - CTES loop ($P_3$)
13. Cooling water circulating pump - Cooling tower loop ($P_4$)
14. Three-ways controlled diverting valve ($V_2$)
15. Closed circuit cooling tower
16. Makeup water
17. Sprayed water pump
18. $NH_3/CO_2$ vapor compression refrigeration machine
19. Refrigerated warehouse (freezing room)
20. $CO_2$ pump
21. Forced-circulation air cooler ($CO_2$ evaporator)
22. Ammonia compressor
23. $NH_3$ / Cooling water heat exchanger ($NH_3$ condenser)
24. $NH_3$ / $CO_2$ heat exchanger ($NH_3$ evaporator; $CO_2$ condenser)
25. Throttling valve
26. Liquid subcooler

**Fig. 2.** Schematic layout of the use of the low-temperature thermal energy recovered from LNG (or bio-LNG) regasification in a satellite terminal for a power plant.

feasibility of a new system configuration that uses the cold recovered to boost the efficiency of vapor-compression chillers. The system proposed will contribute to reducing the carbon footprint of both the LNG supply chain and the food cold chain. Although the paper focuses in particular on *fossil* LNG, the system is compatible with the regasification of more environmentally friendly cryogenic fuels, such as bio-LNG [31], or can even take advantage of the cold thermal energy released from the discharge of LAES.

The paper is organised as follows. After the introduction and the objective, section 2 presents a detailed description of the structure and how the energy plant operates. The selection of the technologies and heat transfer fluids is justified. Then, the modelling is explained and some performance indicators given. The results are presented and discussed in section 3, from a technical and economic perspective. Finally,

**Table 1**
Design simulation parameters.

| Parameter | Value |
|---|---|
| LNG tank temperature ($T_{L0}$), °C | −145 |
| LNG tank pressure ($p_{L0}$), kPa | 328.2 |
| Regasified NG supply temperature ($T_{L6}$), °C | 5 |
| LNG regasification pressure [a], kPa | 800 |
| LNG temperature at the outlet of HE-1 ($T_{L3}$), °C | −70 |
| EG-water inlet/outlet ($T_{E1}$ / $T_{E2}$) temperature in the DBHE, °C | 1 / −5 |
| Temperature of water leaving the heat exchanger HE-2 ($T_{W2}$), °C | 2 |
| Set-point temperature of the CTES (bottoming node), °C | 3 |
| Cooling water inlet/outlet ($T_{W5}$ / $T_{W6}$) temperature in the cooling tower, °C | 37 / 32 |
| Cooling water temperature rise in the ammonia condenser ($T_{WB} - T_{WA}$), °C | 5 |

[a] Gas feed pressure suitable for commercial engines [48].

the conclusions are given in section 4.

## 2. Description and modelling of the system

The energy plant considered in this paper consists of a satellite terminal that supplies gas to a power plant connected to the electrical grid. In this scenario, the electricity generation curve determines the availability of cold from the regasification. A *baseload* power station is assumed: the gas demand is constant, so there is always cold thermal energy available from the regasification site (except in downtime periods). Of the many types of satellite plant, this is one of the most favourable for LNG cold utilization [43].

### 2.1. Description and operation of the system

Fig. 2 shows the schematic layout of the configuration studied. The cold thermal energy released from the regasification process is recovered and exploited for low-temperature refrigeration applications in the cold storage rooms of a neighbouring agro-food industry warehouse.

The scheme proposed maintains the structure and main equipment of a conventional refrigeration system. This is a *non-intrusive* solution that provides a great deal of *operational flexibility* and *reliability* concerning the refrigeration supply. A vapour-compression refrigeration (VCR) machine deals with the thermal load of the cold rooms where frozen foods are kept at −18 °C. The condensation heat of the refrigeration cycle can be rejected through a closed-circuit and mechanical draft cooling tower where the temperature of the cooling medium (water) decreases but is always above the ambient wet-bulb temperature.

The goal of this new configuration is to achieve lower temperatures of the cooling medium, thereby reducing the electricity consumed by the compressor of the VCR machine. This is based on the thermodynamic principle that the efficiency of a refrigeration cycle (expressed by the Energy Efficiency Ratio, *EER*, which is defined as the ratio of the refrigeration capacity to the electricity consumed by compression) enhances as the condensation temperature of the refrigerant decreases.

As shown in Fig. 2, a cold thermal energy storage (CTES) unit is introduced as a low-temperature heat sink to accomplish this efficiency-boosting objective. A kind of underground concrete tank full of water (the most economical thermal fluid because of the large volumes involved), the CTES is indirectly cooled by the LNG cold thermal energy rejected throughout the regasification process in the satellite terminal. Thus, the temperature of the cooling water can be below the ambient air temperature. And unlike wet cooling towers, the CTES operates without continuous consumption of makeup water.

The system operates as follows (Fig. 2). A fraction of the LNG stream (at −145 °C) pumped from the cryogenic tanks (stream L1) goes directly to an ambient air vaporizer (AAV) to be regasified. The remaining fraction is sent to the heat exchanger HE-1 where the LNG indirectly absorbs the heat rejected from the primary heat transfer media (stream E1) pumped by the pump P1. Then, the regasified natural gas is superheated in an AAV. In the heat exchanger HE-2, the primary fluid stream E2 absorbs the sensible heat of the water stream W1 pumped by the pump P2 from the top level of the CTES. Afterwards, the cooled water stream W2 leaving the heat exchanger HE-2 is discharged at the bottom of the CTES to promote thermal stratification.

The energy management of the system is also a critical issue. To avoid further freezing problems, the controller turns off pumps P1 and P2 and closes valve V1 if the bottoming temperature of the tank falls to 2 °C. Once it rises above 4 °C the controller starts up pumps P1 and P2 and reopens valve V1. Notice that whenever valve V1 is closed, the whole stream L1 is sent to an AAV, so the LNG cold thermal energy is fully wasted. In addition, the controller can check at each timestep that streams E1 and W1 are above their freezing point, thus preventing the equipment from being damaged.

The system is also designed to use the CTES as the heat sink of the VCR machine as long as its bottoming temperature is below 11 °C. Thus, the cold-water stream W3 pumped from the bottom of the CTES absorbs the condensation heat from the refrigeration cycle, and the heated-up stream W4 returns to the CTES. However, if the bottoming temperature of the CTES rises above the cut-off limit, the controller turns off pump P3 and starts pump P4, and valve V2 diverts the flow stream WB towards the cooling tower. The objective is to keep the temperature of the CTES low enough to improve the *EER* of the VCR machine. The CTES is again used as a heat sink when its bottoming temperature falls below 7 °C.

### 2.2. Technologies and heat transfer fluids

The chiller used in the configuration presented in Fig. 2 is based on the technology "*NewTon*" developed by Mayekawa Mfg. Co., Ltd. for low-temperature refrigeration applications [55]. It consists of an indirect $NH_3/CO_2$ cascaded system [56]. The ammonia cycle (high-temperature side) includes a double economizer system and a screw compressor.

The use of ammonia ($NH_3$) and carbon dioxide ($CO_2$) has environmental benefits over technologies based on CFCs (e.g., R-12), HCFCs (e.g., R-22) or HFCs (e.g., R-134a or R-404A) that are on the phase-out agenda. But although ammonia has very good thermodynamic features and is widely used in industrial refrigeration installations, it is highly toxic and slightly flammable. The use of $CO_2$ in cascade as the secondary refrigerant flowing through the air coolers (evaporators) in the cold rooms (Fig. 2) keeps the ammonia package in the machine room alone, thereby minimizing its charge in the system. This reduces the risk of an accident if a leak occurs. As refrigerant alternatives, hydrocarbons such as propane can be used with good efficiencies and low environmental impact but safety would be a major concern because of their high flammability. The use of HFO blends (e.g., R-449A) rather than banned refrigerants could also be a very low-GWP solution. Even so, in this paper, a VCR machine running on natural fluids is preferred instead.

The primary heat transfer medium selected in this study is 40%-mass ethylene glycol (EG) – water. Because of the oral toxicity of EG, the primary coolant circuit is installed outside the cold rooms and has no contact with food products. But since the LNG temperature is far below the EG-water freezing point (-24 °C), direct contact between the two fluid streams must be avoided in the heat exchanger HE-1 to prevent crystallization issues. Therefore, a double-bundle heat exchanger could be used [57]. This equipment is a sort of shell-and-tube type heat exchanger with two spiral tube bundles both inside a single shared shell (Fig. 2) [58]. The shell is filled with a fluid (known as *intermediate fluid* or *thermal buffer fluid*) which "*pumps*" the heat from the heating medium (EG-water) to the LNG, thereby preventing freezing. The LNG and the EG-water streams flow inside the top and bottom tube bundle, respectively. The company *Eco-ice Kälte* [45] has developed a patent and technology for this component [59] and has also patented a plant that exploits LNG cold for efficient refrigeration supply in local and remote

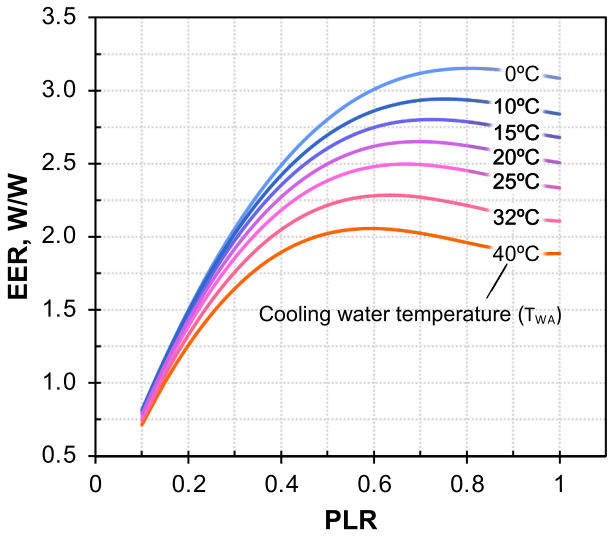


**Fig. 3.** Performance curves of the modelled indirect $NH_3/CO_2$ cascaded vapor-compression refrigeration machine for different PLRs and cooling water temperatures.

areas [60].

Heat transfer fluids such as hydrocarbons or HFCs with a lower freezing point could be an alternative primary heat transfer fluid for more compact heat exchanger technology. The authors shall not discuss them here, however, due to flammability hazards and/or environmental issues. Likewise, carbon dioxide could also be a potential alternative to aqueous glycol solutions but is not considered here because of its higher operating pressure. Ice slurries could also be used [61], although the system proposed discusses the sensible heat of a single-phase heat transfer circuit as in traditional indirect circuits of refrigeration installations.

### 2.3. Modelling and indicators

The different scenarios of satellite LNG plants with waste cold recovery are modelled and simulated in TRNSYS [62] using a typical operating year and a simulation time step of five minutes. Table 1 depicts the design parameters used in the scenarios analysed. The following modelling assumptions are made:

- Thermal and pressure losses are not considered in either equipment or pipes.
- Kinetic and gravitational energies are not considered.
- LNG is assumed to be pure methane for the purpose of calculating thermodynamic properties.
- Leakages of fluids to the environment are neglected.
- The electricity consumption of the fans of the conventional refrigeration machines is not considered.
- The temperature of air in the freezing chambers is assumed to be ideally maintained at the set-point (-18 °C).
- The availability of the system is assumed to be 95%. Different shutdown periods are randomly distributed throughout the year by using TRNSYS Type 1236.

The heat transfer rate in each heat exchanger of the plant is calculated from energy balances and heat transfer equations as follows:

$$\dot{Q} = \dot{m}_i\left(h_{i,in} - h_{i,out}\right) = \dot{m}_j\left(h_{j,out} - h_{j,in}\right) \quad (1)$$

$$\dot{Q} = UA \times \Delta T_m \quad (2)$$

where $UA$ is the overall heat transfer coefficient and $\Delta T_m$ is the effective mean temperature difference between the fluids involved. The energy balance in the underground cold thermal energy storage (CTES, modelled with Type 4) shown in Fig. 2 is calculated as follows:

$$\rho V_{CTES} Cp \frac{dT}{dt} = \dot{m}_{W1} Cp(T_{W2} - T_{W1}) + m_{W3} Cp(T_{W4} - T_{W3}) + \dot{Q}_{gains} \quad (3)$$

The volume of the CTES ($V_{CTES}$) is sized to handle the fraction of the condensation heat released from the VCR machine for the maximum cold that can be recovered from LNG-regasification and for 2.5 h at a temperature range ($\Delta T$) of 6 °C. The heat gain ($\dot{Q}_{gains}$) from the surrounding ground is calculated by assuming that the CTES consists of a 0.5 m thick concrete envelope. The component Type 77 is used to calculate the temperature of the ground. To consider the thermal stratification effect in the CTES, three uniform temperature segments (vertical nodes) are used.

The design temperatures of the liquid $CO_2$ and the ammonia stream leaving the VCR evaporator (see Fig. 2) are –32 °C (saturated liquid) and −35 °C (saturated vapour), respectively. The temperature approach and subcooling in the ammonia condenser are set to 3 °C and 1 °C, respectively. The *EER* (in W/W) of the machine is defined as follows:

$$EER = \frac{\dot{Q}_R}{\dot{W}_{C,el}} = \frac{\dot{Q}_R}{\dot{W}_{C,is}(\eta_{is} \times \eta_m)^{-1}} \quad (4)$$

where $\dot{Q}_R$ is the refrigeration capacity, and $\dot{W}_{C,el}$ and $\dot{W}_{C,is}$ are the electricity input to the motor of the compressor and the isentropic compression power, respectively. The motor efficiency ($\eta_m$) at different part-load ratios ($PLR = \dot{Q}_R/\dot{Q}_{R,peak}$) is based on the technology developed by MYCOM [55]. The variation of the isentropic efficiency ($\eta_{is}$) with the compression ratio is based on the Bitzer OSA.95 compressor series [63]. The modelling of the VCR machine is implemented in TRNSYS through an *EER* polynomial curve given in Fig. 3, which is a function of the cooling water temperature ($T_{WX}$) and the part load ratio (see Appendix A.1.). The nameplate *EER* of the machine is 2.10 W/W [55]. This parameter was used to check that the modelling reproduces the performance of the VCR machine at rated operating conditions.

The total electricity consumed by the refrigeration system of the warehouse ($\dot{W}_{el,R}$) accounts for the electricity consumed by the VCR machine's compressor, the circulating pumps, and the cooling tower (i.e., fan and sprayed water pump). The parasitic electricity consumption of fans or defrosting devices of the cold room air coolers is not considered:

$$\dot{W}_{el,R} = \dot{W}_{C,el} + \sum \dot{W}_P + \dot{W}_{fan,ct} \quad (5)$$

The pumps (modelled with Type 3) are sized by assuming a pressure drop of 10% over the discharge pressure (300 kPa) and an overall efficiency ($\eta_P$) of 80%. As for the cooling tower (closed-circuit and forced draft, modelled with Type 510), the rated fan power ($\dot{W}_{fan,ct}$, in kW) is determined from the following rule of thumb [64]:

$$\dot{W}_{fan,ct} = \dot{m}_{air,design}/21,873 \quad (6)$$

The design air flow rate ($\dot{m}_{air,design}$) is determined from the rated condensation capacity and the design air conditions (i.e., inlet dry-bulb and wet-bulb temperatures of 35 °C and 26 °C, respectively; and leaving wet-bulb temperature and relative humidity of 32 °C and 98%, respectively). As for the make-up water volume ($V_{cw}$, in $m^3$), the following sources of water loss in the cooling tower are considered: evaporation (calculated from Type 510, and assumed to be equivalent to 1% of the sprayed water), drift (assumed to be 0.002% of the sprayed water [65]) and blowdown (taken as 20% of the evaporation rate [64]).

The following *performance indicators* are also defined to evaluate the overall performance of the system:

- The **Cold Recovery Ratio** (*CRR*) is a dimensionless quantity that indicates the amount of LNG cold thermal energy which is transferred in the double-bundle heat exchanger (see Fig. 2) in relation to

the total cold thermal energy released throughout the regasification process:

$$CRR = \frac{\dot{Q}_{DBHE}}{\dot{m}_{LNG}(h_{L6} - h_{L1})} \quad (7)$$

- The **electricity saving** ($\nabla \dot{W}_{el}$) with respect to a conventional reference system ($\dot{W}'_{el,R}$) without LNG cold energy use. Its mathematical expression is as follows:

$$\nabla \dot{W}_{el} = \frac{\dot{W}'_{el,R} - \dot{W}_{el,R}}{\dot{W}'_{el,R}} \times 100\% \quad (8)$$

- The **exergetic efficiency** of the refrigeration installation determines how efficiently the initial physical exergy content of LNG translates into a reduction of the electricity consumed for refrigeration applications. Its mathematical definition is as follows:

$$\eta_{ex} = \frac{\dot{W}'_{el,R} - \dot{W}_{el,R}}{\left(\dot{E}x_{ph,L1} - \dot{E}x_{ph,L6}\right) + \dot{W}_{el,R}} \times 100\% \quad (9)$$

Note that the definition given above sets a conventional regasification system without exergy recovery as the zero-efficiency reference. The physical exergy is calculated as follows: $\dot{E}x_{ph} = \dot{m}[(h - h_0) - T_0(s - s_0)]$. The reference environment is set to 298.15 K and 101.325 kPa.

Finally, the GHG emissions (*GHGe*, in t-$CO_{2,eq}$/year) of the refrigeration system are calculated as follows, using an emission factor (*EF*) of 0.298 kg-$CO_{2,eq}$/kWh:

$$GHGe = EF \times \dot{W}_{el,R} \quad (10)$$

### 2.4. Energy loads forecasting

The LNG regasification rate ($\dot{m}_{LNG}$) is a function of the nameplate electric output of the power plant ($\dot{W}_E$), the lower heating value of natural gas (*LHV*, assumed to be 13.4 kWh/kg), the efficiency of the internal combustion engines ($\eta_{IC}$, set to 47% [66]) and the efficiency of the electric generator ($\eta_{EG}$, set to 95%):

$$\dot{m}_{LNG} = \dot{W}_E \times LHV^{-1} \times \eta_{IC}^{-1} \times \eta_{EG}^{-1} \quad (11)$$

The estimation of the *refrigeration load* of the cold rooms can be based on models developed from the statistical analysis of monitored energy consumption data. However, this method applies only to existing warehouses, and its robustness depends strongly on the quality and time span of these datasets [67]. Another option is to predict the refrigeration load through detailed building modelling and energy simulation programs (e.g., TRNSYS, EnergyPlus, among others). This method is suitable for building design, but it requires detailed information on building geometries, materials, equipment installed, schedules, and so forth.

Since the analysis of a specific warehouse case-study is beyond the scope of this paper, such detailed information or energy demand data are unavailable. Thus, a convenient strategy will be to apply a simplified factor method [68]. In this paper, the hourly refrigeration load profile is predicted from the following dimensionless expression referenced to the peak thermal load ($\dot{Q}_{R,max}$) of the cold rooms:

$$\dot{Q}_R/\dot{Q}_{R,max} = \alpha_1 + \alpha_2 \times \xi + \alpha_3 \times \tau \quad (12)$$

where the factor $\alpha_1$ represents a constant fraction of the thermal load assumed to be 10% (e.g., equipment such as forced air-cooling fans); the factor $\alpha_2$ represents the fraction of the thermal load that depends on the activity schedule of the warehouse (e.g., product load, internal gains such as occupancy or lighting), assumed to be 60%; and the factor $\alpha_3$ accounts for the fraction of the thermal load affected by the outdoor ambient temperature (e.g., transmission heat gains and infiltrations), assumed to be 30%. The weight assigned to the $\alpha$-factors is consistent with the refrigeration load breakdown of typical refrigerated facilities [69].

The activity factor ($0 \leq \xi \leq 1$), also introduced in Eq. (12), is based on the following schedule:

- *Midweek working day*: full activity ($\xi = 1$) from 6:00 to 22:00.
- *Saturday*: full activity ($\xi = 1$) from 6:00 to 14:00.
- *Any other case*: minimum activity ($\xi = 0.1$).

The temperature factor ($0 \leq \tau \leq 1$) in Eq. (12) is defined as the variation of the temperature difference between the outdoor temperature ($T_o$) and the freezing room temperature ($T_r$, −18 °C), with respect to that temperature difference at the design point. Its mathematical expression is as follows:

$$\tau = \frac{T_o - T_r}{T_{o,design} - T_r} \quad (13)$$

Because of its potential for efficiency improvement, the system presented (Fig. 2) will be more attractive for warm than for cold locations. Nonetheless, to quantify and compare the techno-economic potential, and to draw conclusions about opportunities and viability, the simulations performed also include a cold climate case. The three locations selected are representative of a tropical, a Mediterranean, and a continental climate: Bangkok (13.92° N, 100.6° W), Thailand; Tarragona (40.82° N, 0.49° W), Spain; and Oslo (59.90° N, 10.62° W), Norway; respectively. The weather files from the EnergyPlus database are used in the modelling [70]. The 98th percentile outdoor temperature, which is used as the design temperature in Eq. (13), is 35.0, 30.8 and 21.9 °C in Bangkok, Tarragona, and Oslo, respectively.

The **Refrigeration Capacity Index** (*RCI*) is a dimensionless parameter that determines the ratio between the peak refrigeration capacity of a warehouse ($\dot{Q}_{R,max}$) and the maximum low temperature thermal energy that can be recovered from the regasification of the nameplate LNG vaporization capacity of a satellite plant ($\dot{m}_{LNG,np}$). Its mathematical expression is as follows [43]:

$$RCI = \frac{\dot{Q}_{R,max}}{\dot{m}_{LNG,np}(h_{L3} - h_{L2})} \quad (14)$$

### 2.5. Economic analysis

To analyse the economic feasibility of the system (considering a newly built refrigerated warehouse without subsidies or incentives) the indicator used is the **Levelized Cost of Refrigeration** (*LCOR*), in USD/kWh. This parameter indicates the present value of the total cost of producing a unit of refrigeration (i.e., in terms of thermal energy) throughout the system's lifetime. Its mathematical definition is as follows:

$$LCOR = \frac{TCI + \sum_{k=1}^{n}\left[AE_k \times (1+r)^{-k}\right]}{\sum_{k=1}^{n}\left[Q_{R,k} \times (1+r)^{-k}\right]} \quad (15)$$

where $Q_R$ is the refrigeration load (in kWh) throughout year *k*. The parameters *n* and *r* denote the installation lifetime and the annual discount rate, respectively. The Total Capital Investment (*TCI*) of the system is divided into the Fixed Capital Investment (*FCI*), working capital and start-up cost. The *FCI* of the system splits into the Purchased Equipment Cost (*PEC*, assumed to be equal to the free on-board – *FOB* – destination) and other fixed costs (*OFC*, e.g., installation of equipment, piping, instrumentation and control and electric equipment and

**Table 2**
Performance indicators for a Refrigeration Capacity Index equal to unity for the different locations and plant sizes.

| System size [a] | Location | Refrigeration load, GWh/year | Cold recovery from LNG-regasification? [a] | Electricity consumption [b], GWh/year | Water consumption (cooling tower), $m^3$/year | GHG emissions [c], t-$CO_{2,eq}$/year |
|---|---|---|---|---|---|---|
| S | Bangkok | 0.186 | Yes | 0.070 | 43 | 21 |
| | | | No | 0.089 | 485 | 27 |
| | Tarragona | 0.174 | Yes | 0.065 | 25 | 19 |
| | | | No | 0.076 | 436 | 23 |
| | Oslo | 0.166 | Yes | 0.062 | 18 | 19 |
| | | | No | 0.068 | 407 | 20 |
| M | Bangkok | 9.31 | Yes | 3.50 | 2,148 | 1,042 |
| | | | No | 4.46 | 24,263 | 1,330 |
| | Tarragona | 8.71 | Yes | 3.25 | 1,122 | 967 |
| | | | No | 3.79 | 21,794 | 1,128 |
| | Oslo | 8.31 | Yes | 3.11 | 850 | 926 |
| | | | No | 3.42 | 20,326 | 1,021 |
| L | Bangkok | 55.9 | Yes | 21.0 | 12,875 | 6,252 |
| | | | No | 26.8 | 145,577 | 7,978 |
| | Tarragona | 52.3 | Yes | 19.5 | 6,867 | 5,804 |
| | | | No | 22.7 | 130,766 | 6,769 |
| | Oslo | 49.9 | Yes | 18.6 | 5,010 | 5,551 |
| | | | No | 20.5 | 121,957 | 6,123 |

[a] *System sizes*. Power plant electrical output = 50 MW (Small, S); 50 MW (Medium, M); 300 MW (Large, L). Annual LNG-regasification = 0.015 MTPA (Small, S); 0.073 MTPA (Medium, M); 0.44 MTPA (Large, L). Indicator calculated using [b] Eq. (5), [c] Eq. (10), considering an emission factor of 0.298 kg-$CO_{2,eq}$/kWh.

material, among others [71]). The *reference* purchase equipment cost (*PEC*) of the main system components is estimated from the cost functions listed in Table A1. The Chemical Engineering Plant Cost Index (*CEPCI*) annual average composite values are used to update all the original costs obtained in year *y* to the reference year (i.e., 2019):

$$PEC = PEC_y \times \frac{CEPCI_{2019}}{CEPCI_y} \tag{16}$$

The annual expenditures (*AE*) of the system in year *k* are the electricity and water bills, the carbon taxes, and other annual expenditures (*OAE:* maintenance, insurance and taxes and annual overhead costs):

$$AE_k = \left[W_{el,R} \times (C_e + EF \times C_{CO2}) + V_{cw} \times C_w + OAE\right]_k \tag{17}$$

where $W_{el,R}$ is the annual electricity consumed by the refrigeration system (in kWh). The parameters $C_e$, $C_w$ and $C_{CO2}$ represent the electricity tariff, the cost of water and the carbon price, respectively.

The relation below was defined to compare the *LCOR* of the proposed system with that of the conventional system without cold thermal energy recovery from LNG-regasification (*LCOR'*):

$$\Delta LCOR = \frac{LCOR - LCOR'}{LCOR'} \times 100 \tag{18}$$

Note that a negative Δ*LCOR* means an improvement with respect to the conventional system without LNG cold use.

Nevertheless, the parameters involved in the *LCOR* calculation vary widely across locations because they depend on factors such as the electricity mix, climate policies or the particularities of the project. Therefore, assigning them a fixed value is a real challenge. Likewise, the reference purchased equipment costs estimated from the correlations given in Table A1 are a major source of uncertainty. Therefore, a Monte Carlo analysis (sample size, $N = 30{,}000$) was carried out using the MATLAB®-based uncertainty quantification framework UQLab [72] to take into account the impact on the economic feasibility of the uncertainty related to several of these parameters which is depicted in Table A2.

Finally, to evaluate the *economic potential* of the system proposed in this paper, it is defined the indicator **Chances of Economic Feasibility** (*COEF*, in %) which provides information about the number of cases for which the *LCOR* of the LNG cold utilization system is lower – by a factor "*x*" – than that of the conventional refrigeration system in relation to the sample size considered. Its mathematical expression is as follows:

$$COEF = \frac{\sum_{i=1}^{N}\{1if\,\Delta LCOR < x; else 0\}}{N} \times 100\% \tag{19}$$

## 3. Results and discussion

This section presents and analyses the simulation results. The discussion is divided into the technical analysis (section 3.1) and the economic analysis (section 3.2).

### 3.1. Technical analysis

Table 2 shows the electricity and water consumption and GHG emissions for both the systems proposed in this paper (see Fig. 2) and the conventional refrigeration system without cold recovery from LNG-regasification.

The different scenarios considered are set in the climates indicated in section 2.4, and the system sizes are determined by the following electrical output of gas-fired power plants: 1 MW (Small, S), 50 MW (Medium, M) and 300 MW (Large, L). The nameplate vaporization capacity of the satellite terminals that deliver gas to these power units is 223, 11,143 and 66,855 $Nm^3$/h (i.e., 0.17, 8.4, 50 t-LNG/h), respectively. Therefore, the maximum amount of cold thermal energy that can be recovered from LNG-regasification is 29.3 kW, 1.45 MW and 8.71 MW, respectively.

Fig. 4 shows the annual results for the different locations and a medium-size system. A range of refrigeration capacity indexes (see Eq. (14)) in the range 0.25–3 were evaluated. The results are analysed through the dimensionless parameters described in section 2.3, which vary negligibly with plant size. Thus, the conclusions drawn about the technical performance can be extrapolated to any size of the satellite LNG plant. The following observations can be made:

- Fig. 4 (a) shows that as the design refrigeration demand increases in relation to the rated LNG cold thermal energy available, the Cold Recovery Ratio increases, so the amount of cold wasted decreases. The Cold Recovery Ratio is slightly higher in warm climates than in cold climates for *RCIs* $\leq 1$ because of a higher refrigeration load throughout the year. But the influence of the climate on this indicator tends to wear off when the LNG cold thermal energy is fully exploited (i.e., for large *RCIs*). When this is the case, the annual Cold Recovery Ratio reaches ~ 80%, which is equivalent to the maximum

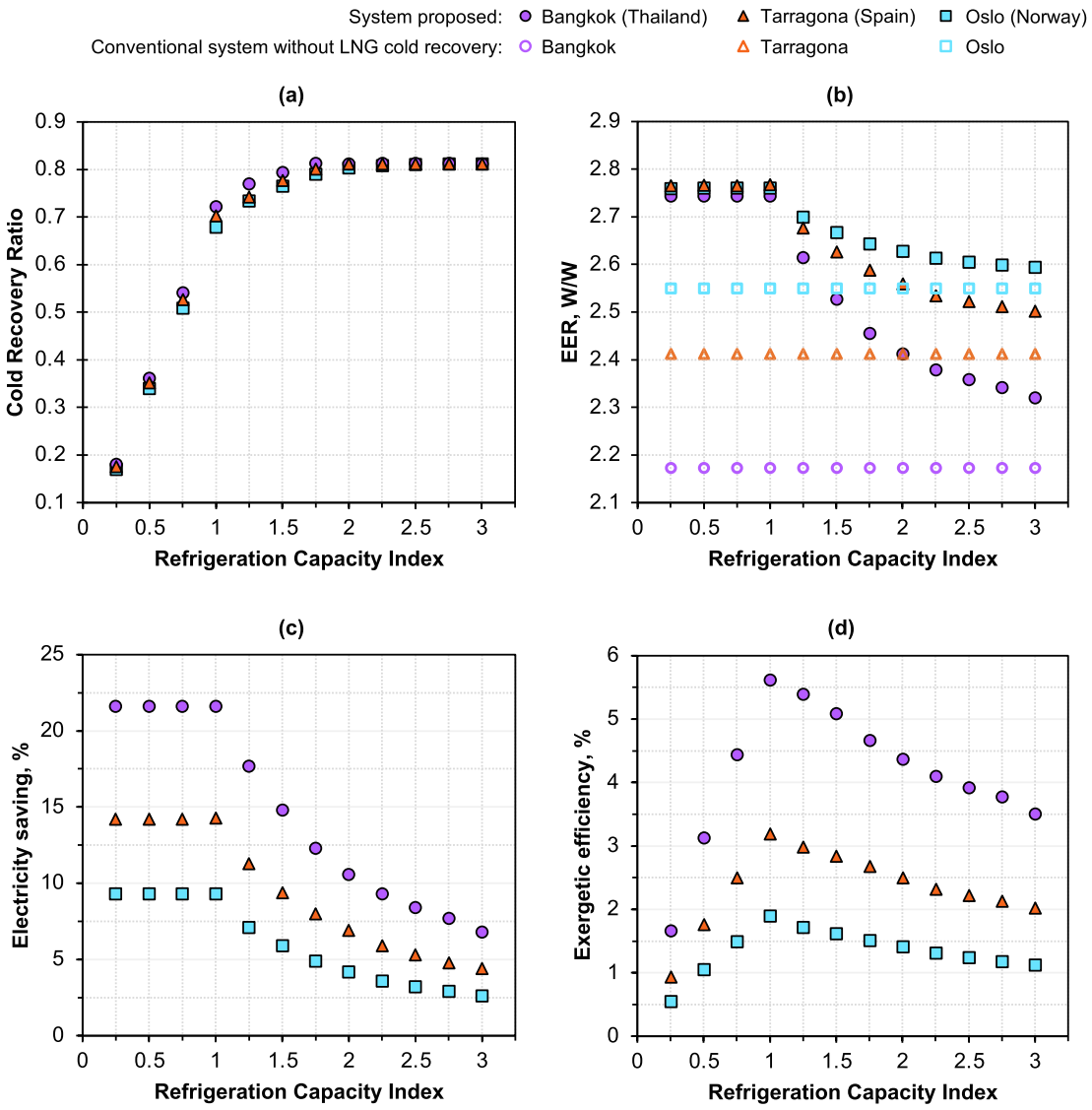


**Fig. 4.** Annual dimensionless results obtained for the refrigeration system with cold recovery from LNG regasification in a satellite plant that supplies gas to a 50 MW electric power plant. Refrigeration capacity indexes in the range 0.25–3 are considered. (a) Cold recovery ratio. (b) Energy Efficiency Ratio (*EER*). (c) Electricity saving. (d) Exergetic efficiency.

LNG cold that can be recovered in the double-bundle heat exchanger of the system configuration proposed in this paper (see Fig. 2).

- Fig. 4 (b) illustrates the annual averaged *EER* of the VCR machine for the system configuration proposed, which is benchmarked against the *EER* for the conventional system. The *EER* monthly results are presented in Fig. 5. The use of LNG cold thermal energy stabilises the condensation temperature of the VCR machine regardless of the weather. Thus, the *EER* is much the same for all the locations considered for *RCIs* $\leq$ 1 (~2.78 W/W). Nonetheless, the enhancement with respect to the conventional system without LNG cold use is much more significant in warm locations. This is because the wet-bulb temperature is usually higher throughout the year, so the water leaves the cooling tower at a higher temperature than in cold locations. As shown in Fig. 5 (a), the performance of the proposed system in Tarragona and Oslo is slightly better in summer because the *PLR* reported is closer to the optimum performance point of the VCR machine (see Fig. 3). In Bangkok, the ambient temperature and the thermal load are quite constant throughout the year, so the same happens for both the *EER* (Fig. 5 (a)) and the *PLR* (Fig. 5 (b)).
- As shown in Fig. 4 (c), the calculated electricity saving is approximately 22%, 14% and 9% in Bangkok, Tarragona and Oslo, respectively, for *RCIs* $\leq$ 1. For example, as shown in Table 2, in a satellite plant that supplies gas to a 50 MW electric power plant and for an *RCI* of 1, the annual electricity savings are 0.96, 0.54 and 0.31 MWh in Bangkok, Tarragona and Oslo, respectively. In the same scenario and locations, 288, 162 and 95 t-$CO_{2,eq}$/year of GHG emissions could be avoided, respectively. However, the *EER* of the VCR machine tends to approach that of the scenario without cold utilization for *RCIs* greater than unity (see Fig. 4 (b)) because the cooling tower is used more often. Hence, the amount of electricity saved decreases sharply once the design refrigeration load exceeds the nameplate LNG cold available.
- Fig. 4 (d) depicts the exergetic efficiencies obtained. Efficiency is highest when the design refrigeration load matches the maximum LNG cold available (i.e., *RCI* = 1). In this case, there is less waste LNG cold thermal energy than for *RCIs* < 1, and more electricity is saved than for *RCIs* greater than 1. On the other hand, the higher the outdoor temperature of a location, the more valuable LNG is as a low-temperature exergy source. The maximum exergetic efficiency found for Bangkok, Tarragona and Oslo is 5.6%, 3.2%, 1.9%, respectively. These efficiencies are very low because the temperature of the water stored in the CTES is much higher than the temperature of LNG. This

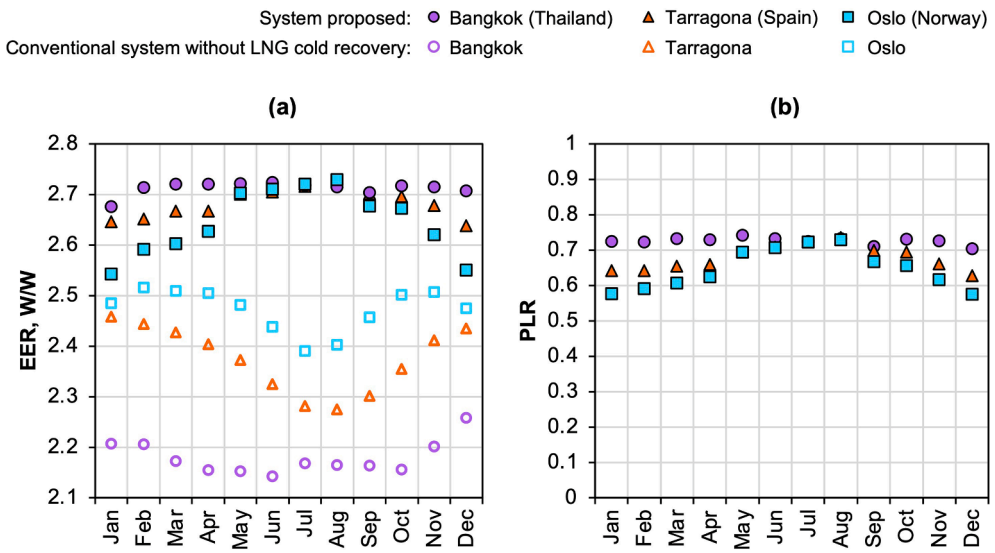


**Fig. 5.** Monthly average results in each location considered for a refrigeration capacity index equal to unity. (a) Energy Efficiency Ratio (*EER*) of the refrigeration machine for the system proposed in this paper and the conventional system without LNG cold utilization. (b) Part load ratio, *PLR* (same for both the proposed and the conventional system).

**Table 3**
Cost breakdown for the base-case scenario and for a Refrigeration Capacity Index equal to unity.

| | Does the refrigeration system exploit the cold thermal energy from LNG-regasification? | | | | | |
|---|---|---|---|---|---|---|
| | Yes | | | No (conventional refrigeration system) | | |
| System size: | S | M | L | S | M | L |
| **• Total Capital Investment (TCI), thousand USD** | **230** | **4,738** | **19,173** | **212** | **4,423** | **17,946** |
| 1. Fixed Capital Investment (FCI): | 192 | 3,948 | 15,978 | 177 | 3,686 | 14,955 |
| *1.1. Purchase Equipment Cost (PEC):* | 132 | 2,704 | 10,944 | 121 | 2,525 | 10,243 |
| 1.1.1. Double-bundle HE (area, $m^2$) | 2 (1.4) | 33 (69) | 117 (417) | 0 (-) | 0 (-) | 0 (-) |
| 1.1.2. EGW/W HE (area, $m^2$) | 6 (2.2) | 77 (109) | 246 (651) | 0 (-) | 0 (-) | 0 (-) |
| 1.1.4. Cold room air coolers (area, $m^2$) | 8 (5.6) | 272 (279) | 1,341 (1,674) | 8 (5.6) | 272 (279) | 1,341 (1,674) |
| 1.1.5. Pumps (power, kW) | 1 (0.42) | 22 (21) | 91 (126) | 0 (0.10) | 5 (4.9) | 22 (29) |
| 1.1.6. Cold thermal energy storage (volume, $m^3$) | 2 (11) | 53 (526) | 267 (3,154) | 0 (-) | 0 (-) | 0 (-) |
| 1.1.7. VCR machine (nameplate refrigeration capacity, kW) | 108 (29.3) | 2,191 (1,450) | 8,707 (8,790) | 108 (29.3) | 2,191 (1,450) | 8,707 (8,790) |
| 1.1.8. Cooling tower (cooling water flow rate, $m^3$/h) | 5 (7.5) | 56 (373) | 174 (2,235) | 5 (7.5) | 56 (373) | 174 (2,235) |
| *1.2. Equipment installation* | 26 | 541 | 2,189 | 24 | 505 | 2,049 |
| *1.3 Piping* | 13 | 270 | 1,094 | 12 | 252 | 1,024 |
| *1.4. Instrumentation and control* | 8 | 162 | 657 | 7 | 151 | 615 |
| *1.5. Electric equipment and material* | 13 | 270 | 1,094 | 12 | 252 | 1,024 |
| 2. Working capital, USD | 29 | 592 | 2,397 | 27 | 553 | 2,243 |
| 3. Start-up cost, USD | 10 | 197 | 799 | 9 | 184 | 748 |
| **• Annual expenses, thousand USD/year** | **15** | **316** | **1,278** | **14** | **295** | **1,196** |
| 1. Operation and maintenance | 12 | 237 | 959 | 11 | 221 | 897 |
| 2. Insurance and taxes | 2 | 39 | 160 | 2 | 37 | 150 |
| 3. Overheads | 2 | 39 | 160 | 2 | 37 | 150 |

*System sizes*. Power plant electric output = 50 MW (Small, S); 50 MW (Medium, M); 300 MW (Large, L). Annual LNG-regasification = 0.015 MTPA (Small, S); 0.073 MTPA (Medium, M); 0.44 MTPA (Large, L).

implies a high exergy destruction rate. Although these efficiencies can be considerably improved by directly exploiting the LNG cold without a VCR machine [43], this option was dismissed to ensure the reliability of the refrigeration supply.

To sum up, the configuration proposed enhances the performance of the conventional refrigeration system without cold recovery from LNG-regasification and does not compromise the supply of cold to the final user. The question that needs to be answered is whether this improvement is large enough to ensure economic competitiveness. The next section analyses how climate and system size affect economic feasibility and conducts a Monte Carlo analysis of the uncertainty of the economic parameters.

### 3.2. Economic potential

Table 3 shows a breakdown of the base-case capital investment and expenses, the electricity and water consumption and the GHG emissions calculated for each of the plant sizes considered and for an *RCI* equal to unity. Table 4 depicts the chances of economic feasibility for each scenario and for different refrigeration capacity indexes. Fig. 6 shows the *LCOR* (Eq. (15)) calculated for the system proposed and its variation with respect to that of the conventional system without cold thermal energy recovery from LNG-regasification (Eq. (18)). The results shown are for an *RCI* equal to unity because, as shown in the previous section, this value gives the best performance reported for the system. As well as the base case and the results obtained from the stochastic simulations, the following favourable and adverse cases are evaluated:

**Table 4**
Chances of Economic Feasibility (*COEF*, in %) calculated for different plant sizes, locations and Refrigeration Capacity Indexes.

| Refrigeration Capacity Index, Eq. (14) | System size | $\Delta LCOR < 0\%$ | | | $\Delta LCOR < -5\%$ | | | $\Delta LCOR < -10\%$ | | |
|---|---|---|---|---|---|---|---|---|---|---|
| | | Bangkok | Tarragona | Oslo | Bangkok | Tarragona | Oslo | Bangkok | Tarragona | Oslo |
| 0.5 | S | 24 | 2 | ~ 0 | ~ 0 | 0 | 0 | 0 | 0 | 0 |
| | M | ~ 100 | 87 | 45 | 61 | 6 | ~ 0 | 5 | 0 | 0 |
| | L | 100 | ~ 100 | 90 | 96 | 40 | 3 | 34 | ~ 0 | 0 |
| 1.0 | S | 45 | 6 | 0.3 | 1.2 | 0 | 0 | ~ 0 | 0 | 0 |
| | M | ~ 100 | 96 | 66 | 79 | 15 | 0.4 | 12 | ~ 0 | 0 |
| | L | 100 | ~ 100 | 97 | 99 | 61 | 8 | 53 | 1.1 | 0 |
| 2.0 | S | 42 | 5 | ~ 0 | ~ 0 | 0 | 0 | 0 | 0 | 0 |
| | M | ~ 100 | 95 | 62 | 17 | ~ 0 | 0 | 0 | 0 | 0 |
| | L | 100 | ~ 100 | ~ 100 | 63 | 2 | 2 | 0 | 0 | 0 |

*System sizes*. Power plant electric output = 50 MW (Small, S); 50 MW (Medium, M); 300 MW (Large, L). Annual LNG-regasification = 0.015 MTPA (Small, S); 0.073 MTPA (Medium, M); 0.44 MTPA (Large, L).

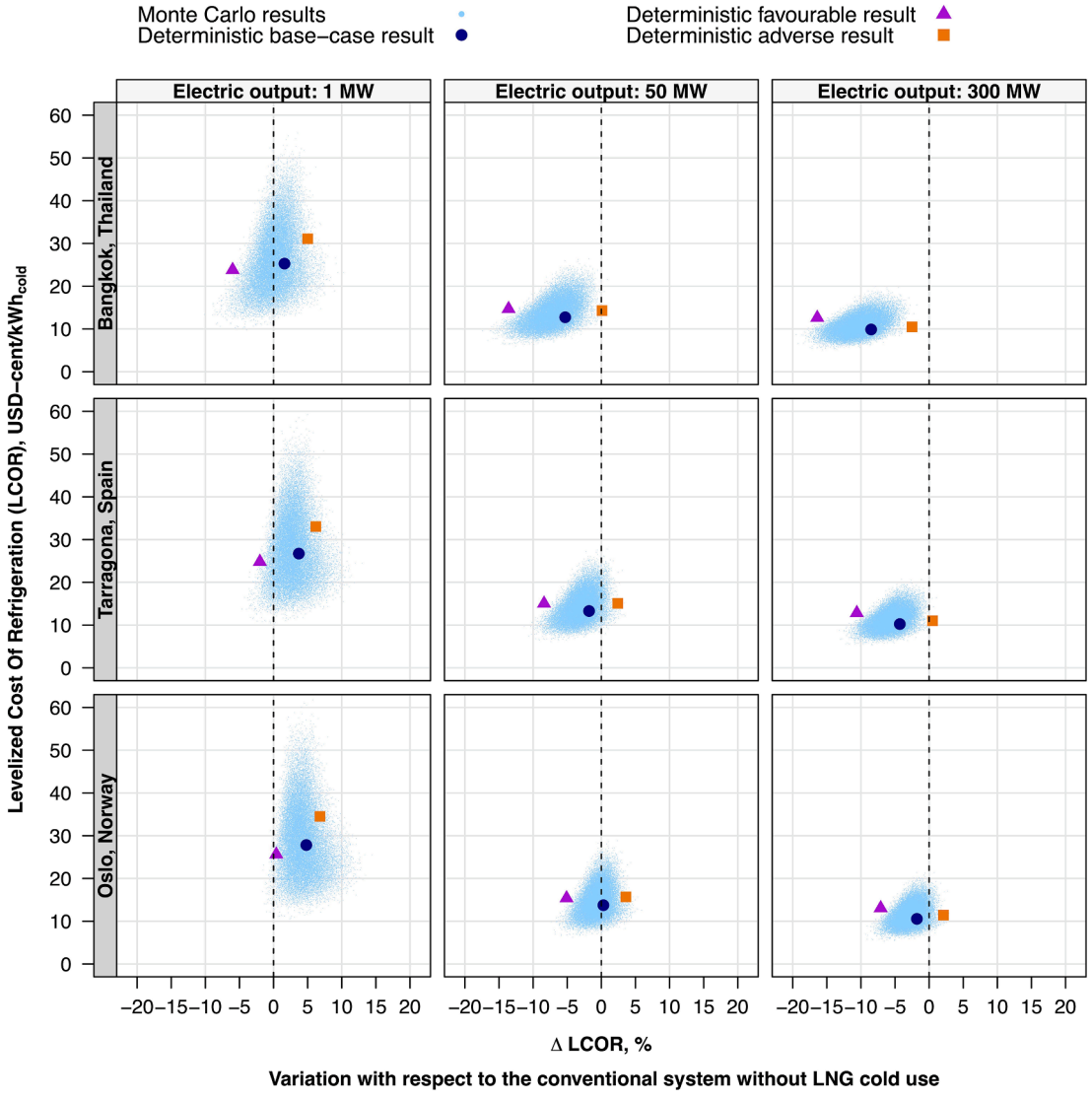


**Fig. 6.** Economic results obtained from simulations for a Refrigeration Capacity Index equal to unity.

- *Favourable case*: Highest plant lifetime of 35 years, lowest discount rate (5%), highest electricity and water tariffs (185.1 USD/MWh and 1.95 USD/$m^3$, respectively), most ambitious carbon tax (119 USD/t-$CO_{2,eq}$).
- *Adverse case*: Plant lifetime of 15 years, highest discount rate (15%), lowest electricity and water tariffs (68.3 USD/MWh and 0.26 USD/$m^3$, respectively), no taxes yet applied to GHG emissions.

Considering all the scenarios evaluated (combinations of climates and plant sizes) and the Monte Carlo results, the *LCOR* estimated for the LNG cold recovery system proposed lies within the stochastic range 0.05–0.50 USD/kWh. As shown in Table 2, the electricity and water consumption and GHG emissions vary proportionally with the size of the system. Nevertheless, the variation of the specific cost of equipment and the specific capital investment with size does not follow a linear trend; instead, it decreases considerably as the equipment capacities increase (Table 3). As shown in Table 4, large LNG cold utilization systems report a chance of economic feasibility above 90%. Economic feasibility is much more unlikely in small plants.

As for the influence of the climate, the following observations can be made:

- As shown in Fig. 6, in cold climates like Oslo the base-case *LCOR* reduction with respect to the conventional refrigeration system is almost negligible or can even be worse. Besides, the chances of achieving *LCOR* reductions above 5% are almost null. At best, the *LCOR* of the conventional configuration may be reduced by 7% for a large plant but only in favourable cases.
- In Mediterranean locations with a climate like Tarragona, the economic perspectives improve slightly. Except for small facilities, it is more likely that the *LCOR* will be lower than that of the conventional system, with a base-case *LCOR* estimated to be 0.12 and 0.11 USD/kWh for medium and large plants, respectively. Indeed, the reduction in the *LCOR* could be around 10% for these plants in a favourable case (Fig. 6). However, the system is unfeasible in the adverse case regardless of the size of the installation.
- Economic performance is best in warm locations like Bangkok. The *LCOR* of the LNG cold utilization system estimated for medium and large plants is around 0.10 USD/kWh. In the favourable case and for these plant sizes, the *LCOR* reduction with respect to the conventional system estimated is above 15%. In particular, for a large plant, the chances of reducing the *LCOR* to 10% are more than 50%, and the system could be feasible even in the adverse case with a refrigeration capacity index equal to one.

Finally, according to the *COEF* values depicted in Table 4, economic competitiveness generally decreases when *RCIs* are above or below one. Despite the specific costs of equipment decrease for larger installations (see Table 3), electricity saving is below the optimum for *RCIs* greater than unity (Fig. 4) and the water consumption is higher as well. On the other hand, although electricity saving is close to the optimum (Fig. 4) when the *RCI* is below unity, the specific cost of equipment increases since the installation needs to be smaller.

## 4. Summary and conclusions

This paper has discussed the main opportunities and bottlenecks of the recovery and use of cold thermal energy as a by-product of LNG-regasification in satellite terminals for sub-zero refrigeration applications in cold rooms of agro-food industries. A novel system configuration has been proposed that aims to use the cold thermal energy to improve the efficiency and sustainability of cascaded vapor-compression refrigeration machines. The technical and economic potential was evaluated using a satellite plant for a base-load power station with cooling recovery for a neighbouring warehouse. The main conclusions drawn are:

- If you aim to use the cold released from LNG-regasification in satellite terminals for foodstuff refrigeration applications, install a back-up refrigeration system or keep the one already installed. The configuration proposed makes the system supplying refrigeration to cold rooms much more reliable and flexible since the conventional operation mode (i.e., using cooling towers) can be used even if there is no LNG cold. The system proposed can also be implemented by making minor modifications to a conventional refrigeration installation. This will make it commercially successful not only in new refrigerated warehouses but also in existing ones.
- The system proposed performs best when the peak refrigeration load of the cold rooms matches the maximum cold thermal energy available from LNG-regasification. For this "*optimal*" case, the electricity savings and greenhouse gas emission reductions were within the range 9–22% with respect to the conventional refrigeration system without LNG cold recovery. The exergetic efficiencies reported were between 1.9 and 5.3%. But as the refrigeration load exceeds the LNG cold available, the performance indicators decline. As for the influence of the climate, the competitiveness of the system improves significantly in tropical climates, owing to the greater efficiency-boosting effect with respect to the conventional refrigeration system.
- The economic prospects are optimistic for medium/large-size systems and temperate/warm climates. In advantageous scenarios, the cost of producing refrigeration over the system's lifetime is between 0.07 and 0.20 USD/kWh, which means a 5–15% reduction with respect to the conventional refrigeration system without LNG cold recovery. In contrast, in cold locations the system is less economically competitive because the energy savings are poor. In the future, the economic feasibility of the system should be determined by considering the economic and climatic parameters of the specific location where a project will be executed. The refrigeration load of cold rooms must also be monitored or simulated to estimate the energy savings accurately.

### CRediT authorship contribution statement

**Antonio Atienza-Márquez:** Conceptualization, Methodology, Software, Validation, Formal analysis, Investigation, Writing - original draft, Writing - review & editing, Writing - review & editing, Visualization. **Joan Carles Bruno:** Conceptualization, Writing - review & editing, Supervision. **Alberto Coronas:** Project administration, Conceptualization, Supervision.

### Declaration of Competing Interest

The authors declare that they have no known competing financial interests or personal relationships that could have appeared to influence the work reported in this paper.

### Acknowledgements

Antonio Atienza-Márquez acknowledges the financial support received from the Ministerio de Ciencia, Innovación y Universidades (MICINN) of Spain for the pre-doctoral contract No. FPU15/04514 between the academic years 2016-17 and 2019-20. Mr. John F. Bates, coordinator of the language service at the Universitat Rovira i Virgili, is acknowledged for his editing contribution to the final version of the manuscript.

## Appendix A

### A.1. Energy efficiency Ratio

The polynomial curve used to calculate the Energy Efficiency Ratio (*EER*, in W/W) of the cascaded $NH_3/CO_2$ vapor-compression refrigeration machine modelled in the paper is given from the following polynomial equation, which is a function of the part lo1ad ratio (PLR) and the cooling water temperature ($T_{WA}$):

$$EER(PLR,T_{WA}) = a_0 + a_1 \times PLR + a_2 \times T_{WA} + a_3 \times PLR^2 + a_4 \times PLR \times T_{WA} + a_5 \times T_{WA}^2 + a_6 \times PLR^3 + a_7 \times PLR^2 \times T_{WA} + a_8 \times PLR \times T_{WA}^2 + a_9 \times T_{WA}^3 + a_{10} \times PLR^4 + a_{11} \times PLR^3 \times T_{WA} + a_{12} \times PLR^2 \times T_{WA}^2 + a_{13} \times PLR \times T_{WA}^3 + a_{14} \times T_{WA}^4$$

The coefficients of the equation above are the following:

$a_0 = 0.001841$; $a_1 = 8.709$; $a_2 = 0.002173$; $a_3 = -5.937$; $a_4 = 0.02419$; $a_5 = -0.0002589$; $a_6 = -1.412$; $a_7 = -0.1037$; $a_8 = -0.00145$; $a_9 = 8.328 \times 10^{-6}$; $a_{10} = 1.722$; $a_{11} = 0.06035$; $a_{12} = 0.0007863$; $a_{13} = 9.803 \times 10^{-6}$; $a_{14} = -7.922 \times 10^{-8}$

### A.2. Economics

Table A1 depicts the functions used to estimate the purchase cost of the main components of the configuration presented in Fig. 2. Table A2 shows the uncertainties related to the parameters involved in the economic analysis.

**Table A1**
Cost functions (in USD) used to determine the reference purchased cost of the main system components.

| System component | Purchase cost function (USD) | Source |
|---|---|---|
| - Pumps (including motor) | $1{,}120 \times \dot{W}_{(kW)}^{0.8}$ | [73] |
| - Double-bundle heat exchanger (HE-1) [a] | $2{,}661.3 \times A_{(m^2)}^{0.71}$ | [74] |
| - Heat exchanger HE-2 [a] | $6{,}014.2 \times A_{(m^2)}^{0.65}$ | [74] |
| - Cold thermal energy storage [b] | $177.2 \times V_{CTES,(m^3)}^{0.9}$ | [75] |
| - Cold room air coolers [a] | $1{,}397.0 \times A_{(m^2)}^{0.89}$ | [76] |
| - VCR machine [c] | $3{,}918.2 \times Q_{R,(kW)}^{0.77} \times F_T$ | [74] |
| - Cooling tower | $1{,}038.5 \times V_{cw,(m^3/h)}^{0.63}$ | [76] |

[a] Overall heat transfer coefficients (*U*) used to estimate the heat transfer area of heat exchangers: 0.2 kW/($m^2$·K) for the double-bundle heat exchanger HE-1; 3 kW/($m^2$·K) for the heat exchanger HE-2 and the 0.5 kW/($m^2$·K) for the cold room air coolers.
[b] Correlation adjusted by the factor 1.21 for Euro to USD conversion.
[c] Evaporator temperature factor ($F_T$): 3.36 (–33 °C).

**Table A2**
Inputs for the Levelized Cost of Refrigeration (*LCOR*) calculation considering uncertainties.

| Input | Base values | Distributions [a] | Notes |
|---|---|---|---|
| System lifetime (n), years | 25 | N [25, 3.33] | Typical |
| Discount rate (r), % | 10 | U [5, 15] | Typical [77] |
| Electricity tariff ($C_e$), USD/MWh | 102.0 | T [68.3, 185.1, 102.0] | Typical [78] |
| Cost of water ($C_w$), USD/$m^3$ | 0.89 | T [0.26, 1.95, 0.89] | Typical [79] |
| Carbon tax ($C_{CO2}$), USD/t-$CO_{2,eq}$ | 10 | T [0, 119, 10] | Typical [80] |
| Equipment cost (*PEC*) [b], USD | $PEC_{ref}$ | U [0.5, 1.5] × $PEC_{ref}$ | Estimated |
| Other fixed costs (*OFC*) [c], USD | $OFC_{ref} = 0.46 \times PEC$ | T [0.25, 1.75, 1.00] × $OFC_{ref}$ | Estimated |
| Working capital and start-up cost (*WSC*) [d], USD | $WSC_{ref} = 0.20 \times FCI$ | T [0.25, 1.75, 1.00] × $WSC_{ref}$ | Estimated |
| Other annual expenditures [e] (*OAE*), USD | $OAE_{ref} = 0.08 \times FCI$ | T [0.25, 1.75, 1.00] × $OAE_{ref}$ | Estimated |

[a] Nomenclature used for distributions. U [a, b]: Uniform distribution between a and b: T [a, b, c]: Triangular distribution with minimum value a, maximum value b and likeliest value c; N [μ, σ]: Normal is a normal distribution with mean value μ and standard deviation σ.
[b] The uncertainties apply individually to each of the cost functions depicted in Table A1.
[c] Base values for fixed costs (other than the purchased equipment costs) [71]: Equipment installation = 20% of PEC; Piping = 10% of PEC; Instrumentation and control = 6% of PEC; Electric equipment and material = 10% of PEC.
[d] Base values for the working capital and the start-up cost [71]: 10% and 5% of FCI, respectively.
[e] Base values for the maintenance, the insurance and taxes, and the annual overheads: 6%, 1% and 1% of FCI, respectively.

## References


[1] United Nations Framework Convention on Climate Change (UNFCCC). The Paris Agreement 2015. http://unfccc.int/paris_agreement/items/9485.php (accessed March 30, 2019).
[2] International Energy Agency (IEA). Gas Market Report, Q2-2021 2021. https://www.iea.org/reports/gas-market-report-q2-2021.
[3] International Group of Liquefied Natural Gas Importers (GIIGNL). GIIGNL Annual Report 2021 2021. https://giignl.org/publications.
[4] Atienza-Márquez A, Bruno JC, Coronas A. Cold recovery from LNG-regasification for polygeneration applications. Appl Therm Eng 2018;132:463–78. https://doi.org/10.1016/j.applthermaleng.2017.12.073.
[5] He T, Chong ZR, Zheng J, Ju Y, Linga P. LNG cold energy utilization: Prospects and challenges. Energy 2019;170:557–68. https://doi.org/10.1016/j.energy.2018.12.170.
[6] Pospíšil J, Charvát P, Arsenyeva O, Klimeš L, Špiláček M, Klemeš JJ. Energy demand of liquefaction and regasification of natural gas and the potential of LNG for operative thermal energy storage. Renew Sustain Energy Rev 2019;99:1–15. https://doi.org/10.1016/j.rser.2018.09.027.
[7] Romero Gómez M, Ferreiro Garcia R, Romero Gómez J, Carbia CJ. Review of thermal cycles exploiting the exergy of liquefied natural gas in the regasification process. Renew Sustain Energy Rev 2014;38:781–95. https://doi.org/10.1016/j.rser.2014.07.029.
[8] Sun Z, Zhao Q, Wu Z, Lin K. Thermodynamic comparison of modified Rankine cycle configurations for LNG cold energy recovery under different working conditions. Energy Convers Manag 2021;239:114141. https://doi.org/10.1016/j.enconman.2021.114141.
[9] Khor JO, Dal Magro F, Gundersen T, Sze JY, Romagnoli A. Recovery of cold energy from liquefied natural gas regasification: Applications beyond power cycles. Energy Convers Manag 2018;174:336–55. https://doi.org/10.1016/j.enconman.2018.08.028.
[10] Mehrpooya M, Moftakhari Sharifzadeh MM, Rosen MA. Optimum design and exergy analysis of a novel cryogenic air separation process with LNG (liquefied natural gas) cold energy utilization. Energy 2015;90:2047–69. https://doi.org/10.1016/j.energy.2015.07.101.
[11] Qi M, Park J, Kim J, Lee I, Moon I. Advanced integration of LNG regasification power plant with liquid air energy storage: Enhancements in flexibility, safety, and power generation. Appl Energy 2020;269:115049. https://doi.org/10.1016/j.apenergy.2020.115049.
[12] Song C, Liu Q, Deng S, Li H, Kitamura Y. Cryogenic-based CO2 capture technologies: State-of-the-art developments and current challenges. Renew Sustain Energy Rev 2019;101:265–78. https://doi.org/10.1016/j.rser.2018.11.018.
[13] Sultan H, Muhammad HA, Bhatti UH, Min GH, Baek IH, Baik Y-J, et al. Reducing the efficiency penalty of carbon dioxide capture and compression process in a natural gas combined cycle power plant by process modification and liquefied natural gas cold energy integration. Energy Convers Manag 2021;244:114495. https://doi.org/10.1016/j.enconman.2021.114495.
[14] Gao T, Lin W, Gu A. Improved processes of light hydrocarbon separation from LNG with its cryogenic energy utilized. Energy Convers Manag 2011;52:2401–4. https://doi.org/10.1016/j.enconman.2010.12.040.
[15] Li S, Wang B, Dong J, Jiang Y. Thermodynamic analysis on the process of regasification of LNG and its application in the cold warehouse. Therm Sci Eng Prog 2017;4:1–10. https://doi.org/10.1016/j.tsep.2017.08.001.
[16] International Institute of Refrigeration (IIR). Future data centre cooled using waste cooling from LNG Terminal in Singapore 2021. https://iifiir.org/en/news/future-data-centre-cooled-using-waste-cooling-from-lng-terminal-in-singapore (accessed July 1, 2021).
[17] Eghtesad A, Afshin H, Kazemzadeh HS. Energy, exergy, exergoeconomic, and economic analysis of a novel power generation cycle integrated with seawater desalination system using the cold energy of liquified natural gas. Energy Convers Manag 2021;243:114352. https://doi.org/10.1016/j.enconman.2021.114352.
[18] Emadi MA, Pourrahmani H, Moghimi M. Performance evaluation of an integrated hydrogen production system with LNG cold energy utilization. Int J Hydrogen Energy 2018;43:22075–87. https://doi.org/10.1016/j.ijhydene.2018.10.048.
[19] Ayou DS, Eveloy V. Energy, exergy and exergoeconomic analysis of an ultra low-grade heat-driven ammonia-water combined absorption power-cooling cycle for district space cooling, sub-zero refrigeration, power and LNG regasification. Energy Convers Manag 2020;213:112790. https://doi.org/10.1016/j.enconman.2020.112790.
[20] Atienza-Márquez A, Bruno JC, Akisawa A, Nakayama M, Coronas A. Fluids selection and performance analysis of a polygeneration plant with exergy recovery from LNG-regasification. Energy 2019;176:1020–36. https://doi.org/10.1016/j.energy.2019.04.060.
[21] Fang Z, Shang L, Pan Z, Yao X, Ma G, Zhang Z. Exergoeconomic analysis and optimization of a combined cooling, heating and power system based on organic Rankine and Kalina cycles using liquified natural gas cold energy. Energy Convers Manag 2021;238:114148. https://doi.org/10.1016/j.enconman.2021.114148.
[22] Ghorbani B, Ebrahimi A, Ziabasharhagh M. Novel integrated CCHP system for generation of liquid methanol, power, cooling and liquid fuels using Kalina power cycle through liquefied natural gas regasification. Energy Convers Manag 2020;221:113151. https://doi.org/10.1016/j.enconman.2020.113151.
[23] Atienza-Márquez A, Bruno JC, Akisawa A, Coronas A. Performance analysis of a combined cold and power (CCP) system with exergy recovery from LNG-regasification. Energy 2019;183:448–61. https://doi.org/10.1016/j.energy.2019.06.153.
[24] Biscardini G, Schmill R, Del Maestro A. Small going big. Why small-scale LNG may be the next big wave. Strategy & (Part of the PwC network). 2017.
[25] Strantzali E, Aravossis K, Livanos G, Chrysanthopoulos N. A Novel Multicriteria Evaluation of Small-Scale LNG Supply Alternatives: The Case of Greece. Energies 2018;11:903. https://doi.org/10.3390/en11040903.
[26] Fioriti D, Baccioli A, Pasini G, Bischi A, Migliarini F, Poli D, et al. LNG regasification and electricity production for port energy communities: Economic profitability and thermodynamic performance. Energy Convers Manag 2021;238:114128. https://doi.org/10.1016/j.enconman.2021.114128.
[27] International Gas Union (IGU) Program Commitee (PGC) D3. Small Scale LNG. 2015.
[28] International Gas Union (IGU). Flexible LNG Facilities Enhancing Functionality Across the LNG Value Chain. 27th World Gas Conf., Washington DC (USA): 2018.
[29] Kanagawa T. Japan's LNG Utilization and Environmental Efforts. Tokyo (Japan) 2008.
[30] Basel Agency for Sustainable Energy (BASEL), International Energy Agency (IEA), SEAD. Webinar series: How Cooling as a Service is set to revolutionise the cooling industry 2020.
[31] Naquash A, Qyyum MA, Haider J, Lim H, Lee M. Renewable LNG production: Biogas upgrading through CO2 solidification integrated with single-loop mixed refrigerant biomethane liquefaction process. Energy Convers Manag 2021;243:114363. https://doi.org/10.1016/j.enconman.2021.114363.
[32] Xu W, Duan J, Mao W. Process study and exergy analysis of a novel air separation process cooled by LNG cold energy. J Therm Sci 2014;23:77–84. https://doi.org/10.1007/s11630-014-0679-5.
[33] Xu W, Huang Z, Fan S. Optimized Analysis of Cold Energy Utilization for Cold Storage Project of Xingtan LNG Satellite Station. In: Dincer I, Midilli A, Kucuk H, editors. Prog. Exergy, Energy, Environ., Cham: Springer International Publishing; 2014, p. 569–76. 10.1007/978-3-319-04681-5_53.
[34] Lin W, Zhang N, Gu A. LNG (liquefied natural gas): A necessary part in China's future energy infrastructure. Energy 2010;35:4383–91. https://doi.org/10.1016/j.energy.2009.04.036.
[35] Roszak EA, Chorowski M. Exergy analysis of combined simultaneous Liquid Natural Gas vaporization and Adsorbed Natural Gas cooling. Fuel 2013;111:755–62. https://doi.org/10.1016/j.fuel.2013.03.074.
[36] Ning J, Sun Z, Dong Q, Liu X. Performance study of supplying cooling load and output power combined cycle using the cold energy of the small scale LNG. Energy 2019;172:36–44. https://doi.org/10.1016/j.energy.2019.01.094.
[37] Kanbur BB, Xiang L, Dubey S, Choo FH, Duan F. Thermoeconomic assessment of a micro cogeneration system with LNG cold utilization. Energy 2017;129:171–84. https://doi.org/10.1016/j.energy.2017.04.071.
[38] Kanbur BB, Xiang L, Dubey S, Choo FH, Duan F. Thermoeconomic and environmental assessments of a combined cycle for the small scale LNG cold utilization. Appl Energy 2017;204:1148–62. https://doi.org/10.1016/j.apenergy.2017.01.061.
[39] Kanbur BB, Xiang L, Dubey S, Choo FH, Duan F. Thermoeconomic analysis and optimization of the small scale power generation and carbon dioxide capture system from liquefied natural gas. Energy Convers Manag 2019;181:507–18. https://doi.org/10.1016/j.enconman.2018.11.077.
[40] Kanbur BB, Xiang L, Dubey S, Choo FH, Duan F. Finite sum based thermoeconomic and sustainable analyses of the small scale LNG cold utilized power generation systems. Appl Energy 2018;220:944–61. https://doi.org/10.1016/j.apenergy.2017.12.088.
[41] Kanbur BB, Xiang L, Dubey S, Choo FH, Duan F. Life-cycle-integrated thermoeconomic and enviroeconomic assessments of the small-scale-liquefied natural gas cold utilization systems. Int J Energy Res 2019;43:4104–26. https://doi.org/10.1002/er.4510.
[42] Zhao L, Dong H, Tang J, Cai J. Cold energy utilization of liquefied natural gas for capturing carbon dioxide in the flue gas from the magnesite processing industry. Energy 2016;105:45–56. https://doi.org/10.1016/j.energy.2015.08.110.
[43] Atienza-Márquez A. Exergy recovery from LNG-regasification for polygeneration of energy, PhD Thesis. Tarragona (Spain): Universitat Rovira i Virgili, 2020. http://www.tdx.cat/handle/10803/670489.
[44] Kälte-Klima-Sachsen GmbH n.d. http://kaelte-klima-sachsen.de/ (accessed December 11, 2019).
[45] Eco ice Kaelte GmbH n.d. http://www.eco-ice.net/en/ (accessed August 16, 2021).
[46] LNGcold solutions GmbH 2019. http://lngcold.energy/ (accessed December 5, 2019).
[47] Wärtsilä. Small-and medium-scale LNG terminals 2018.
[48] Punnonen K. Small and Medium size LNG for Power Production. Power Plant: Wärtsilä Finl Oy, Finl; 2013. p. 1–18.
[49] Asia Pacific Energy Research Centre (APERC). Small-scale LNG in Asia-Pacific. Asia-Pacicifc Economic Cooperation (APEC); 2019.
[50] The Carbon Trust. The Emerging Cold Economy. Sustainable solutions for rapidly increasing cooling needs. 2015.
[51] Nomura Research Institute. Study on Opportunities and Issues in introducing mini LNG facilities and equipments in Indonesia 2015.
[52] Strantzali E, Aravossis K, Livanos GA. Evaluation of future sustainable electricity generation alternatives: The case of a Greek island. Renew Sustain Energy Rev 2017;76:775–87. https://doi.org/10.1016/j.rser.2017.03.085.
[53] Carron F. Small Scale LNG Based Power Generation in the Philippines. Power Genp Asia 2014, 2014..
[54] New LNG power plant at Gibraltar powered by MAN Energy Solutions 2019. https://www.man-es.com/discover/gibraltar-builds-a-modern-lng-power-plant (accessed November 30, 2019).

[55] Mayekawa MFG. Co. L. NewTon 2009. https://mayekawa.com/lp/newton/ (accessed August 13, 2020).
[56] Asano H, Mugabi N. Actual Energy Conservations By Using NH3/CO2 refrigeration system. Int. Conf. Sav. Energy Refrig. Air-Conditioning, Jeollanam-Do (South Korea): 2013, p. ICSERA2013-3-C–2.
[57] Pineda Quijano D, Infante Ferreira C, Duivenvoorden W, Mieog J. Noortgaete T Van Der, Velpen B Van Der. Techno-economic feasibility study of a system for the transfer of refrigeration capacity from LNG regasification plants to industrial assets. 12th IEA Heat Pump Conf. Rotterdam 2017.
[58] Atienza-Márquez A, Ayou DS, Carles Bruno J, Coronas A. Energy polygeneration systems based on LNG-regasification: Comprehensive overview and techno-economic feasibility. Therm Sci Eng Prog 2020;20:100677. https://doi.org/10.1016/j.tsep.2020.100677.
[59] Braun R, Otto P. Method and heat exchanger for recovering cold during re-gasification of cryogenic liquids. WO 2017/114518, 2017.
[60] Braun R, Peter O, Bihl L. Refrigeration supply plant coupled to regasification apparatus of a Liquefied Natural Gas terminal. WO 2019/020135, 2019.
[61] Hawlader MNA, Wahed MA. Analyses of ice slurry formation using direct contact heat transfer. Appl Energy 2009;86:1170–8. https://doi.org/10.1016/j.apenergy.2008.11.003.
[62] TRNSYS 2017. http://www.trnsys.com/ (accessed March 19, 2020).
[63] BITZER GmbH. Ammonia compressor packs - ACP Series 2018.
[64] Leeper SA. Wet Cooling Towers: "Rule-Of-Thumb" Design and simulation. 1981.
[65] Hall S. Cooling Towers. Branan's Rules Thumb Chem. Eng., Elsevier; 2012, p. 182–9. 10.1016/B978-0-12-387785-7.00010-4.
[66] Wärtsilä. Wärtsilä 50DF multi-fuel engine 2019.
[67] Ji Y, Xu P, Duan P, Lu X. Estimating hourly cooling load in commercial buildings using a thermal network model and electricity submetering data. Appl Energy 2016;169:309–23. https://doi.org/10.1016/j.apenergy.2016.02.036.
[68] Duanmu L, Wang Z, Zhai ZJ, Li X. A simplified method to predict hourly building cooling load for urban energy planning. Energy Build 2013;58:281–91. https://doi.org/10.1016/j.enbuild.2012.11.029.
[69] ASHRAE. ASHRAE Handbook-Refrigeration - SI Edition. 2014.
[70] EnergyPlus - Weather Data 2019. https://energyplus.net/weather (accessed December 10, 2019).
[71] Bejan A, Tsatsaronis G, Moran M. Thermal Design and Optimization. Jonh Wiley & Sons, Inc.; 1996.
[72] Marelli S, Sudret B. UQLab: A Framework for Uncertainty Quantification in MATLAB. 2nd Int. Conf. Vulnerability Risk Anal. Manag. (ICVRAM 2014), University of Liverpool, United Kingdom: 2014, p. 2554–63. 10.1061/9780784413609.257.
[73] Dorj P. Thermoeconomic Analysis of a New Geothermal Utilization CHP Plant in Tsetserleg, Mongolia. University of Iceland, 2005.
[74] Woods DR. Rules of Thumb in Engineering Practice. Wiley 2007. https://doi.org/10.1002/9783527611119.
[75] Sveinbjörnsson D, Linn P, Jensen L, Trier D, Hassine I Ben, Jobard X. D2.3 - Large Storage Systems for DHC Networks. Fifth generation, low temperature, high exergy district heating and cooling networks (FLEXYNETS). 2017.
[76] Smith R. Chemical Process Design and Integration. John Wiley & Sons, Ltd 2005. https://doi.org/10.1529/biophysj.107.124164.
[77] Heck N, Smith C, Hittinger E. A Monte Carlo approach to integrating uncertainty into the levelized cost of electricity. Electr J 2016;29:21–30. https://doi.org/10.1016/j.tej.2016.04.001.
[78] International Energy Agency (IEA). Electricity Information: Overview (2020 Edition). Data Publ Stat Rep 2020:1–10.
[79] United States Department of Energy. Water and Wastewater Annual Price Escalation Rates for Selected Cities across the United States. 2017.
[80] World Bank Group. State and Trends of Carbon Pricing October 2020. Washington DC (USA): 2020.